

# UC Irvine

## UC Irvine Previously Published Works

### Title

Implementation and Performance of the Seeded Reconstruction for the ATLAS Event Filter Selection Software

### Permalink

<https://escholarship.org/uc/item/7060x0xj>

### ISBN

9780780391833

### Authors

Santamarina, C  
Muiño, P Conde  
dos Anjos, A  
et al.

### Publication Date

2005

### DOI

10.1109/rtc.2005.1547532

### Copyright Information

This work is made available under the terms of a Creative Commons Attribution License, available at <https://creativecommons.org/licenses/by/4.0/>

Peer reviewed

# Implementation and Performance of the Seeded Reconstruction for the ATLAS Event Filter Selection Software

C. Santamarina<sup>||</sup>, P. Conde Muiño<sup>||</sup>, A. dos Anjos<sup>\*</sup>, S. Armstrong<sup>†</sup>, J.T.M. Baines<sup>‡</sup>, C.P. Bee<sup>§</sup>, M. Biglietti<sup>¶</sup>, J.A. Bogaerts<sup>||</sup>, M. Bosman<sup>\*\*</sup>, B. Caron<sup>††</sup>, P. Casado<sup>\*\*</sup>, G. Cataldi<sup>‡‡</sup>, D. Cavalli<sup>x</sup>, G. Comune<sup>xi</sup>, G. Crone<sup>xii</sup>, D. Damazio<sup>†</sup>, A. De Santo<sup>xiii</sup>, M. Diaz Gomez<sup>xiv</sup>, A. Di Mattia<sup>xv</sup>, N. Ellis<sup>||</sup>, D. Emeliyanov<sup>‡</sup>, B. Epp<sup>xvi</sup>, S. Falciano<sup>xv</sup>, H. Garitaonandia<sup>\*\*</sup>, S. George<sup>xiii</sup>, A. Gesualdi Mello<sup>xxii</sup>, V. Ghete<sup>xvi</sup>, R. Goncalo<sup>xiii</sup>, J. Haller<sup>||</sup>, S. Kabana<sup>xvii</sup>, A. Khomich<sup>||</sup>, G. Kilvington<sup>xii</sup>, J. Kirke<sup>‡</sup>, N. Konstantinidis<sup>xii</sup>, A. Kootz<sup>xix</sup>, A.J. Lankford<sup>xx</sup>, A. Lowe<sup>xiii</sup>, L. Luminari<sup>xv</sup>, T. Maeno<sup>†</sup>, J. Masik<sup>xxi</sup>, C. Meessen<sup>§</sup>, R. Moore<sup>††</sup>, P. Morettini<sup>xxiii</sup>, A. Negri<sup>xxiv</sup>, N. Nikitin<sup>xv</sup>, A. Nisati<sup>xv</sup>, C. Osuna<sup>\*\*</sup>, C. Padilla<sup>||</sup>, N. Panikashvili<sup>xxvi</sup>, F. Parodi<sup>xxiii</sup>, E. Pasqualucci<sup>xv</sup>, V. Perez Reale<sup>xvii</sup>, J.L. Pinfold<sup>††</sup>, P. Pinto<sup>||</sup>, Z. Qian<sup>§</sup>, S. Resconi<sup>x</sup>, S. Rosati<sup>||</sup>, C. Sánchez<sup>\*\*</sup>, D.A. Scannicchio<sup>xxiv</sup>, C. Schiavi<sup>xxiii</sup>, E. Segura<sup>\*\*</sup>, J.M. de Seixas<sup>xxii</sup>, S. Sivoklov<sup>xxv</sup>, A. Sobreira<sup>||</sup>, R. Soluk<sup>††</sup>, E. Stefanidis<sup>xii</sup>, S. Sushkov<sup>\*\*</sup>, M. Sutton<sup>xii</sup>, S. Tapprogge<sup>xxvii</sup>, S. Tarem<sup>xxvi</sup>, E. Thomas<sup>xvii</sup>, F. Touchard<sup>§</sup>, G. Usai<sup>xxviii</sup>, B. Venda Pintoc<sup>xxix</sup>, A. Ventura<sup>‡‡</sup>, V. Vercesi<sup>xxiv</sup>, T. Wengler<sup>||</sup>, P. Werner<sup>||</sup>, S.J. Wheeler<sup>††</sup>, F.J. Wickens<sup>‡</sup>, W. Wiedenmann<sup>\*</sup>, M. Wieler<sup>‡</sup> and G. Zoernig<sup>\*</sup>

**Abstract**—ATLAS is one of the four LHC experiments that will start data taking in 2007, designed to cover a wide range of physics topics. The ATLAS trigger system has to cope with a rate of 40 MHz and 23 interactions per bunch crossing. It is divided in three different levels. The first one (hardware based) provides a signature that is confirmed by the the following trigger levels (software based) by running a sequence of algorithms and validating the signal step by step, looking only to the region of the space indicated by the first trigger level (seeding). In this presentation, the performance of one of these sequences that run at the Event Filter level (third level) and is composed of clustering at the calorimeter, track reconstruction and matching, will be presented.

<sup>\*</sup>Department of Physics, University of Wisconsin, Madison, Wisconsin, USA; <sup>†</sup>Brookhaven National Laboratory (BNL), Upton, New York, USA; <sup>‡</sup>Rutherford Appleton Laboratory, Chilton, Didcot, UK; <sup>§</sup>Centre de Physique des Particules de Marseille, IN2P3-CNRS-Université d'Aix-Marseille 2, France; <sup>¶</sup>Dipartimento di Fisica dell'Università degli studi di Napoli 'Federico II' e I.N.F.N., Napoli, Italy; <sup>||</sup>CERN, Geneva, Switzerland <sup>\*\*</sup>Institut de Física d'Altes Energies (IFAE), Universidad Autónoma de Barcelona, Barcelona, Spain; <sup>††</sup>University of Alberta, Edmonton, Canada; <sup>‡‡</sup>Dipartimento di Fisica dell'Università di Lecce e I.N.F.N., Lecce, Italy; <sup>x</sup>Dipartimento di Fisica dell'Università di Milano e I.N.F.N., Milan, Italy; <sup>xi</sup>Department of Physics and Astronomy, Michigan State University, East Lansing, MI 48824, USA; <sup>xii</sup>Department of Physics and Astronomy, University College London, London, UK; <sup>xiii</sup>Department of Physics, Royal Holloway, University of London, Egham, UK; <sup>xiv</sup>Section de Physique, Université de Genève, Switzerland; <sup>xv</sup>Dipartimento di Fisica dell'Università di Roma 'La Sapienza' e I.N.F.N., Rome, Italy; <sup>xvi</sup>Institut für Experimentalphysik der Leopold-Franzens Universität, Innsbruck, Austria; <sup>xvii</sup>Laboratory for High Energy Physics, University of Bern, Switzerland; <sup>xviii</sup>Lehrstuhl für Informatik V, Universität Mannheim, Mannheim, Germany; <sup>xix</sup>Fachbereich Physik,

Bergische Universität Wuppertal, Germany; <sup>xx</sup>University of California at Irvine, Irvine, USA; <sup>xxi</sup>Institute of Physics, Academy of Sciences of the Czech Republic, Prague, Czech Republic; <sup>xxii</sup>Universidade Federal do Rio de Janeiro, COPPE/EE, Rio de Janeiro, Brazil; <sup>xxiii</sup>Dipartimento di Fisica dell'Università di Genova e I.N.F.N., Genoa, Italy; <sup>xxiv</sup>Dipartimento di Fisica Nucleare e Teorica dell'Università di Pavia e INFN, Pavia, Italy; <sup>xxv</sup>Institute of Nuclear Physics, Moscow State University, Moscow, Russia; <sup>xxvi</sup>Department of Physics, Technion, Haifa, Israel; <sup>xxvii</sup>Institut für Physik, Universität Mainz, Mainz, Germany; <sup>xxviii</sup>Dipartimento di Fisica dell'Università di Pisa e I.N.F.N. Pisa, Italy; <sup>xxix</sup>CFNUL - Universidade de Lisboa, Faculdade de Ciências, Lisbon, Portugal.

## I. INTRODUCTION

ATLAS is one of the two multi-purpose experiments of the LHC. This accelerator will provide, at its design luminosity of  $10^{34} \text{ cm}^{-2} \text{ s}^{-1}$ , an average of 23 inelastic proton-proton collisions per bunch crossing at a center of mass energy of 14 TeV. This means a rate of  $10^9$  interactions per second. The ATLAS Trigger must reduce this to a rate of the order of 200 Hz which is the maximum storage capacity of the Data Acquisition System with the highest possible efficiency over the potentially interesting events.

The ATLAS trigger is structured in three levels. The first one (LVL1) is fully accomplished by electronic modules that detect electron, photon, jet, missing  $E_T$  and muon signatures. This system also provides the time reference for the rest of the subsystems. LVL1 must, in a latency of 10 ms, reduce the rate to 75 kHz. The second and third levels of the ATLAS trigger constitute the so-called High Level Trigger (HLT). Both levels

analyze the events accepted by LVL1 in commercial computer farms.

In particular the third trigger level, called Event Filter (EF) is expected to have a mean execution time of 1 second. Both the second and Event Filter levels are seeded, this means guided by the corresponding previous level to access data only in a possible interesting region of the space called Region of Interest (RoI). The access to one or several isolated regions in the same event is the origin of the main difference between reconstruction algorithms in the ATLAS Event Filter and the offline.

The possibility to define trigger menus combining different event signatures that originated in a variable number of RoIs and the execution of the algorithms by the Trigger Steering will be described in section III.

A particularity of ATLAS is that, even though the above commented differences with the pure offline algorithms, the programming environment is common for both projects and in fact the aim is that EF algorithms are adaptations of the offline ones sharing many of the tools with the advantage avoiding double coding.

In this paper we will review the design and implementation of a fully seeded Event Filter slice for selection of high transverse momentum isolated electrons and photons. We will go through the different algorithms that take part in the slice, their goals as well as their time performance. We will also see which is the global behavior of the slice to select some event samples.

## II. $e - \gamma$ SELECTION

There are several objectives of isolated electron and photon selection, from electromagnetic calorimeters and trigger calibration channels to the discovery of supersymmetric particles. However, there is a major goal which is the discovery of the Higgs boson through one of its different decays leading to electrons and photons. In table I a summary of some relevant channels with electron or photon participation is shown together with their corresponding trigger signature. A trigger signature is just a label to tag events that fulfill several conditions. For example,  $2e15i$  labels an event where two different RoI's produced an electromagnetic shower over certain cuts that matched a reconstructed track with some characteristics, as described in section IV. This event has high probability of having two isolated electrons/positrons with initial transverse energy above  $25 \text{ GeV}/c$ .

## III. THE HIGH LEVEL TRIGGER STEERING

As commented in the introduction, the ATLAS High Level Trigger (HLT) is guided by the first level (LVL1) hardware based trigger. The HLT only accesses data in an RoI whose position is initially provided by LVL1 and incidentally refined by the successive HLT algorithms. The HLT algorithms are driven by the High Level Trigger Steering (the Steering from now on). The Steering is a top algorithm of the ATLAS software project (ATHENA). It steers algorithm execution based on existing active Trigger Elements combinations and

TABLE I  
PHYSICS GOALS OF THE  $e/\gamma$ S DETECTION

Selection signature	Examples of physics coverage
$e25i$	$W \rightarrow e\nu, Z \rightarrow ee,$ top production, $W', Z',$ $H \rightarrow WW^*/ZZ^*$
$2e15i$	$Z \rightarrow ee, H \rightarrow WW^*/ZZ^*$
$\gamma60i$	direct photon production, $H \rightarrow \gamma\gamma$
$2\gamma20i$	$H \rightarrow \gamma\gamma$
$\mu10 + e15i$	$H \rightarrow WW^*/ZZ^*, \text{SUSY}$

information from Sequences. A Trigger Element is a boolean object which a High Level Trigger algorithm outputs after execution. The algorithms also receive an input Trigger Element from the previous algorithm in the Sequence. The Steering only executes an algorithm if the input Trigger Element is active. The Sequence is therefore a three column list where every row contains an algorithm in the central column between its corresponding input and output Trigger element names. An algorithm can link an object of any type to its output Trigger Element and the subsequent algorithms will be able to retrieve this object navigating through the chain of Trigger Elements produced by the preceding algorithms and up to the LVL1 RoI descriptor (an object that summarizes the relevant information from LVL1, in particular the position of the RoI). The Steering configuration is completed with a signature file. A signature is a requirement of one or more active trigger elements. The Steering is programmed to provide early rejection of impossible signatures and hence optimizing the time performance of the High Level Trigger (we will see more below).

The High Level Trigger Algorithms are classified in two types:

- On one side we have the Feature Extraction Algorithms that in general retrieve and unpack detector data and create simple classes composed of meaningful physics variables. They are time consuming algorithms and should be run as less as possible. For example, the algorithm called TrigCaloRec retrieves the cells within and RoI from the ATLAS calorimeters and constructs Calorimeter Electromagnetic Clusters with them. The Calorimeter Cluster class contains, among others, the position of the cluster and its energy.

In some cases a Feature Extraction algorithm only merges information already retrieved by a previous algorithm. As an example we can consider TrigegammaRec. This algorithm retrieves, via the Trigger Elements chain, the clusters created by TrigCaloRec and the tracks created by the corresponding Inner Detector algorithm and performs the best track-cluster match building-up several variables as  $E/P$ , the quotient between the cluster energy and the track momentum. The Feature Extraction algorithms always leave active their output Trigger Element.

- The second type of High Level Trigger Algorithms are the Hypothesis algorithms. These are extremely fast execution algorithms ( $\sim 1\mu s$ ) who retrieve the physics information from the Trigger Element chain and validate a hypothesis. They either set active their output Trigger element if the hypothesis conditions are fulfilled or leave it inactive.

The idea behind this scheme is that the same time consuming Feature Extraction algorithm can be used to provide several fast Hypothesis algorithms with the required physics information where the cuts will be applied. This will avoid double execution of Feature Extraction algorithms in the same RoI. Let us consider the Event Filter sequence to validate the signatures  $e25i$  and  $e15i$ , isolated single electrons of 25 and 15 GeV  $E_T$ . Both will need, for example, the same information from the calorimeter. Then, TrigCaloRec, the above mentioned calorimeter Feature Extraction Algorithm, will be executed once in the RoI. The output Trigger Element will drive two different hypothesis algorithms to the same electromagnetic cluster to whom they will apply their cuts.

The High Level Trigger Steering decides upon event fate at every step based on the information from the required Signatures of a trigger menu. This means that for example, if a required signature of an event is  $2e15i$  (two isolated electrons with transverse energy higher than 15 GeV) then the algorithm execution will check at every sequence step that there are two independent candidates of this type. If at some point there is only one, the steering will immediately reject the event. This means that the algorithm execution by the steering is not made independently for every RoI. On the contrary, all the initial RoI algorithm sequences are started in parallel from the initial LVL1 input and the signatures dependencies checked at every step. This implementation optimizes time consumption of the High Level Trigger avoiding execution of unnecessary algorithms. An example will be explained in the next two sections.

#### IV. THE SEEDED EVENT FILTER $e - \gamma$ SLICE

The ATLAS collaboration has a wide software program for electron and photon reconstruction. The aim of coupling the High Level Trigger software project in the global reconstruction project was to benefit from the reconstruction work already made and not to repeat twice the same code. Moreover, future maintenance and improvement of the algorithms will be guaranteed. To the date, performance studies of the Event Filter have been made based on offline reconstruction. However, the use of the HLT steering forces to make an effort to adapt the existing code to be used in the High Level Trigger. The access to data only in small parts of the detector as well as the multiple execution of an algorithm for the same event (once per RoI) are two of the major problems to solve. The approach is quite different to that of Level 2 where specific trigger algorithms have been developed for which the time performance was the priority. In these conditions we have been able to set up a full Event Filter slice where offline tools are used for the physics objects reconstruction with access

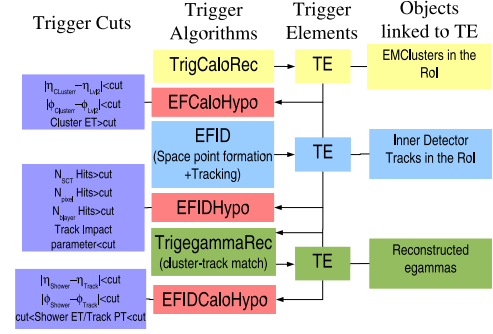


Fig. 1. Scheme of the Event Filter Seeded Slice

restricted to the RoI detector data and executed by the steering. This slice consists of the following algorithms:

- TrigCaloRec: this is, as already mentioned, a clustering algorithm for the electromagnetic calorimeter. It also accesses data in the hadronic calorimeter to compute energy leakage of electromagnetic showers or identify and veto hadrons.
- EFID: which is not a single algorithm but composed of:
  - Pixel clustering: retrieves data from the Pixel silicon detector and forms clusters in the RoI.
  - SCT clustering: retrieves data from the Silicon Tracker detector and forms clusters in the RoI.
  - TRT drift circles: retrieves data from the Transition Radiation Tracker and forms drift circles in the RoI.
  - Space Point formation: uses the clusters and drift circles from the previous algorithms and forms space points (hit positions).
  - iPatRec: a tracking algorithm based on Pattern Recognition [1].
- TrigegammaRec: is an algorithm that reconstructs the so called egamma objects in the RoI. An egamma object is composed of three types of variables:
  - Electromagnetic Shower variables.
  - The best matching track with the shower (if exists) variables.
  - Combined Shower and Track variables.

The slice is completed with the corresponding Hypothesis algorithms where selection cuts are applied. We describe below the applied selection requirements.

- EFCaloHypo: is the Event Filter Calorimeter hypothesis algorithm. It performs a geometrical cut on  $|\eta_{Cluster} - \eta_{LVL2}| < cut$  and  $|\phi_{Cluster} - \phi_{LVL2}| < cut$ , where the subscript  $LVL2$  indicates the RoI position received from LVL2, and a cut on the cluster  $E_T > cut$ .
- EFIDHypo: performs the cuts on the inner detector variables. The number of space points in the different detectors must fulfill  $N_{pixel} Hits \geq cut$ ,  $N_{SCT} Hits \geq cut$  and  $N_{b-layer} Hits \geq cut$ . Finally the Track-impact parameter  $< cut$  rejects events not produced near enough to the interaction point.

TABLE II  
SELECTION CUTS FOR THE  $e25i$  AND THE  $e15i$  SIGNATURES

Algorithm	Signature	Selection Requirement
<b>EFCalo</b>	$e25i$ or $e15i$	$ \eta_{Cluster} - \eta_{LVL2}  < 0.2$
<b>EFCalo</b>	$e25i$ or $e15i$	$ \phi_{Cluster} - \phi_{LVL2}  < 0.2$
<b>EFCalo</b>	$e25i$	$E_T > 22$ GeV
<b>EFCalo</b>	$e15i$	$E_T > 15$ GeV
<b>EFID</b>	$e25i$ or $e15i$	$N_{SCTHits} \geq 7$
<b>EFID</b>	$e25i$	$N_{pixelHits} \geq 1$
<b>EFID</b>	$e25i$	$N_{b-layerHits} \geq 1$
<b>EFIDCalo</b>	$e25i$ or $e15i$	$ \eta_{Cluster} - \eta_{Track}  < 0.1$
<b>EFIDCalo</b>	$e25i$ or $e15i$	$ \phi_{Cluster} - \phi_{Track}  < 0.2$
<b>EFIDCalo</b>	$e25i$	$0.8 < E/P < 1.3, \eta < 1.37$
<b>EFIDCalo</b>	$e25i$ or $e15i$	$0.7 < E/P < 2.5, \eta > 1.37$
<b>EFIDCalo</b>	$e15i$	$0.7 < E/P < 1.7, \eta < 1.37$

- **EFIDCaloHypo**: performs a cut on the Cluster-Track residual  $|\eta_{Cluster} - \eta_{Track}| < cut$  and  $|\phi_{Cluster} - \phi_{Track}| < cut$  and on the ratio between the cluster energy and the track reconstructed momentum  $lower - cut < E/P < upper - cut$ . In this case two different  $\eta$  regions are defined where two different lower and upper cuts are applied.

Two different sets of requirements have been applied to identify isolated electrons with transverse energy higher than 15 GeV and higher than 25 GeV respectively corresponding to the so-called  $e15i$  and  $e25i$  signatures. The values can be consulted in table II for both signatures.

## V. PERFORMANCE OF THE SLICE

The performance of the presented slice should report three parameters. One is the efficiency over a wished sample of data, the second is the rejection power of the reducible physics background and the third the average processing time. The main source of reducible background is composed of jet-jet events where one or both jets are misidentified as electrons [2]. Unfortunately, the reduction factor is so high that a large Monte Carlo event sample needs to be produced in order to make a calculation. This production is currently being made and hence, no rejection factors are yet produced with the seeded slice. The used selection cuts correspond to an optimization where the offline approach (no-seeded) was used [1].

For the efficiencies of the algorithms two different samples were used. The first one consists of single electron events with monochromatic transverse energy of 25 GeV. This sample is an artificial construction to optimize the selection of the  $e25i$  signature, useful for some of the physics goals listed in table I. The second sample we have considered is the  $Z \rightarrow e^+e^-$  decay. For this channel the High Level Trigger Steering with two simultaneous signatures,  $e25i$  and  $2e15i$ , was tested for the first time. As commented above, the  $2e15i$  signature is an "and" of two independent  $e15i$  signatures. The used cuts were those optimized with the offline and

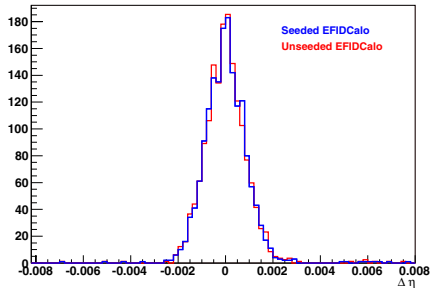
TABLE III  
ALGORITHM EFFICIENCIES. THE VALUES ARE WITH RESPECT TO THE PREVIOUS ALGORITHM OUTPUT. THE "ALL" ROW ACCOUNTS FOR THE TOTAL OF THE THREE ALGORITHMS. THE INPUT SAMPLE ARE EVENTS WHERE TWO ROIS ARE PASSED BY LVL2.

Sample	25 GeV Single e	$Z \rightarrow ee$	$Z \rightarrow ee$	$Z \rightarrow ee$
Signature	$e25i$	$e25i$	$2e15i$	$2e15i + e25i$
<b>EFCalo</b>	98.9%	97.7%	71.2%	99.9%
<b>EFID</b>	92.2%	96.7%	82.8%	95.9%
<b>EFIDCalo</b>	96.0%	94.6%	94.0%	95.2%
<b>All</b>	87.5%	89.4%	55.5%	91.2%

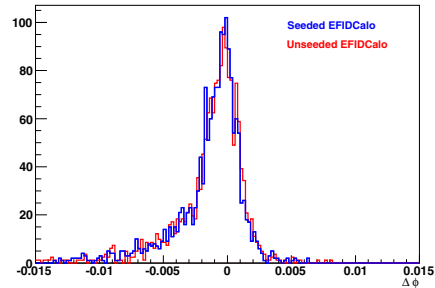
hence, further improvement will be expected soon but in the meanwhile, the efficiency results are shown in table III where for every algorithm the result is computed as the number of active output Trigger Elements divided by the number of active Trigger Elements from the previous algorithm in the Sequence. The exception is the  $2e15i$  signature where the efficiency is accounted as events with two active output Trigger Elements from a given algorithm divided by the number of events with two active Trigger Elements from the previous algorithm. In the  $Z \rightarrow e^+e^-$  sample it was requested that from LVL2 there were at least two active Trigger Elements in order to have the same amount of events for both signatures.

Concerning time consumption, the reconstruction at Event Filter takes much less than the total average allowed time of 1 second. In table IV we can see the time consumption per algorithm and in figure 2 the integrated distribution for the full slice where the data unpacking contribution is explicitly shown. The times are per RoI while 1.4 RoI are expected in average per event in ATLAS running conditions [1]. They were calculated with a 2.8 GHz processor and extrapolated to the expected run conditions of 8 GHz or equivalent multicore hardware. The data used for this time estimation is a jet-jet data sample in the nominal design luminosity of  $10^{34} \text{ cm}^{-2}\text{s}^{-1}$  and accounting for pile-up effects. The use of a dijet sample is justified on the basis that they constitute the bulk of the rate. However, in future studies the effect of rate reduction due to rejection by the first algorithms should be accounted. This effect reduces the average processing time per event. The short time consumption opens up new possibilities in the use of the Event Filter which could lead to efficiency increase. Nevertheless, this subject needs further study that we are tackling now.

On the other hand, an exhaustive comparison of the reconstruction quality of the seeded algorithms slice has been performed with the offline results. Energy resolution in the calorimeter, momentum resolution in the Inner detector, position resolution in both systems and matching residual have shown to be comparable to the results obtained by the standard offline  $e/\gamma$ s reconstruction. As an example, in figures 3(a) and 3(b) we show the comparison between the  $\eta$  and  $\phi$  residuals of the calorimeter cluster and inner detector track



(a) Cluster Calorimeter/Inner Detector Track  $\eta$  residual



(b) Cluster Calorimeter/Inner Detector Track  $\phi$  residual

Fig. 3.

TABLE IV

EVENT FILTER EXECUTION TIME PER ROI. THE PERFORMANCE IS EXTRAPOLATED TO THE FUTURE HARDWARE CONDITIONS.

	Unpacking		Total	
	Time (ms)	RMS	Time (ms)	RMS
TrigCaloRec	2.3	0.5	5.0	0.9
SCT cluster.	0.8	0.5	1.7	1.0
Pixel cluster.	0.6	0.4	1.7	1.1
TRT drift c.	1.8	1.2	3.6	2.2
SP formation	—	—	5.8	3.8
iPatRec	—	—	18.4	21.2
ID prost proc	—	—	3.1	2.2
TriggammaRec	—	—	15.2	2.3

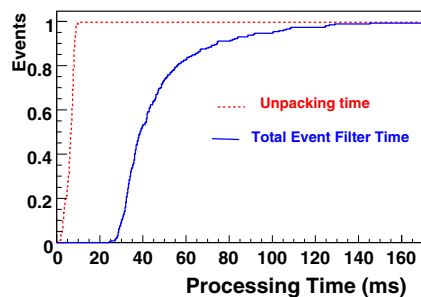


Fig. 2. Integrated distribution of the Event Filter execution time.

match at the electromagnetic calorimeter level.

## VI. CONCLUSION

For the first time a full slice of trigger algorithms has been implemented for high  $P_T$  electrons and photons selection in the ATLAS experiment. The performance of this slice executed by the High Level Trigger Steering has been tested. The tests include the requirement of two simultaneous signatures in the event which has been made for the first time with physics algorithms. This analysis approach will permit a better

understanding of the trigger menus and improvements in its performance.

## ACKNOWLEDGMENT

We wish to thank the organization of the IEEE Real Time 2005 workshop for their exceptional work and all the help for presenting our work.

## REFERENCES

- [1] ATLAS Collaboration. ATLAS High-Level Trigger Data Acquisition and Controls Technical Design Report. *CERN/LHCC/2003-022 ATLAS TDR* 16 June 2003.
- [2] ATLAS Collaboration. ATLAS Detector and Physics Performance Technical Design Report. *CERN/LHCC/99-15 ATLAS TDR* 15 May 1999.
- [3] Gesualdi Mello, Aline et al. Overview of the High-Level Trigger Electron and Photon Selection for the ATLAS Experiment at the LHC. IEEE Real Time 2005 Conference 2005
- [4] Gianluca Comune. Trigger Menus and Steering. PESA Performance session at 2005 May Software Week <http://agenda.cern.ch/fullAgenda.php?ida=a052747>